JOURNAL OF THE KOREAN ASTRONOMICAL SOCIETY
31: 117 ~ 125, 1998

OBSERVATIONS OF HC_3N TOWARD THE SGR B2 MOLECULAR CLOUD

Y. C. MINH AND HYUN-GOO KIM
Korea Astronomy Observatory, Hwaam, Yusŏng, Taejŏn 305-348
(Received Sep. 22, 1998; Accepted Oct. 15, 1998)

ABSTRACT

We have observed the 10−9 transitions of HC_3N and its ^{13}C substitutes ($H^{13}CCCN$, $HC^{13}CCN$, and $HCC^{13}CN$), and the vibrationally excited 12−11 (v_7=1) HC_3N transition toward the Sgr B2 molecular cloud. The observed HC_3N emission shows an elongated shape around the Principal Cloud (~4.5 pc in R.A. × 7.4 pc in Decl.). The optically thin $H^{13}CCCN$ line peaks around the (N) core and we derive the total column density $N(H^{13}CCCN) = 4 \times 10^{13}$ cm^{-2} at this position. Toward the 2′ N cloud which shows the peculiar chemistry, the HC_3N lines show enhancements compared to the extended envelope. The shocks of the 2′ N may have resulted in the enhancement of HC_3N. The hot component of HC_3N is strongly concentrated around the (N) core and its HPW is ~0.9 pc in diameter. We derive the lower limit of the abundance ratio $N(HC_3N)/N(H^{13}CCCN)$ to be larger than 40 in most regions except the (M) and (N) cores. The fractionation processes of ^{13}C at this region may not be as effective as previously reported.

Key Words : ISM:abundances - ISM:individual(Sgr B2) - ISM:molecules

I. INTRODUCTION

The Sgr B2 molecular cloud locates near our Galactic center at a distance of 8.5 kpc from us. This cloud represents a relatively extreme case of high-luminosity star formation taking place in a very massive giant molecular cloud and is one of the most extensively studied regions in the Galaxy. This cloud has a total mass of ~ 5×10^7 $M_\odot$ and a size of ~40 pc in diameter. The extended envelope, which contains ~90% of the total mass, has a mean density, $n(H_2) = 5 \times 10^3$ cm^{-3}. This mean density is very high compared to the averaged value for the GMCs in the Galactic plane by more than an order of magnitude. Sgr B2 is a very active star forming region. The observed infrared luminosity is about 7×10^6 $L_\odot$, but the true luminosity is expected to be a factor of 10 higher than this value (Thronson & Harper 1986). In the central region of the cloud there exist a major gas component, the Principal Cloud, of a size of ~ 5 − 10 pc in diameter and a mean density of $n(H_2) = 3 - 30 \times 10^4$ cm^{-3} (Scoville, Solomon, & Penzias 1975; Irvine, Goldsmith, & Hjalmarson 1987, hereafter IGH). Interferometric observations reveal that there exist ~50 compact H II regions having newly born massive stars along the north-south direction 'inside' the Principal Cloud, named as Sgr B2(M), (N), and (S) (cf. Gordon *et al.* 1993). A large body of extensive studies for Sgr B2 has been focused on these three compact core components.

The molecular line studies have revealed that Sgr B2 is an extremely rich source of complex molecules; in fact, some molecules have been detected only in Sgr B2 (e.g., Cummins, Linke, & Thaddeus 1986; Nummelin *et al.* 1998). The previous studies have suggested that Sgr B2 is a complicated system and consisted of various clumps whose physical and chemical properties may be different largely with each other. For instance, there exists another gas clump at the 2′N position which is prominent in some specific molecules such as, for example, HNCO and HCO_2^+ (Wilson *et al.* 1996; Minh *et al.* 1998). This 2′N cloud has a size of ~7 pc in diameter and a total mass of 1.7×10^5 $M_\odot$, but it may not have dense cores to excite heavy molecules to be detected. This cloud may have resulted from a large-scale collapsing motion, which appears as the red-shifted and blue-shifted components with the projected velocities of about ±30 km s^{-1}, symmetrically located around the 2′N position (Minh *et al.* 1998). At the 1.5′ south from the (M) position there seems to be another gas cloud, the Southern Cloud, which could be a separated component near Sgr B2. This Cloud seems not showing any chemical peculiarity such as the 2′N cloud (Minh & Hjalmarson 1998).

The overall density structure of Sgr B2, however, has not been well known mainly due to the large distance from us and large H_2 column densities along the lines of sight (~ 1×10^{24} cm^{-2} through the cores) (e.g., IGH; Goldsmith *et al.* 1987). We have made observations of the millimeter-wave transitions of HC_3N and its isotope varients toward Sgr B2 to study the physical and chemical properties of Sgr B2. The observations are described in §2, observed results in §3, and discussions in §4.

II. OBSERVATIONS

Observations were carried out using the 15 m Swedish ESO telescope (SEST[1]) on La Silla, Chile, in April 1997. The telescope is described in Booth *et al.*

SEST is operated by Onsala Space Observatory, the Swedish National Facility for Radio Astronomy, with financial support from the Swedish Natural Science Research Council (NFR) and ESO.

Table 1. Column densities of HC_3N and $H^{13}CCCN$ in 4 positions.

Positions[a]	(0, 0)	(0, 0.75)	(0, 1.5)	(0, 2.25)
$\int T_R^*(HC_3N)dV$ [Kkms^{-1}] [b]	134.8	130.9	136.4	108.0
$\int T_R^*(H^{13}CCCN)dV$ [Kkms^{-1}]	3.5	9.7	3.1	0.7
$N(HC_3N)$ [cm^{-2}][c]	$2.2\pm1.0\times10^{16}$	$1.7\pm0.8\times10^{16}$	$1.9\pm0.9\times10^{16}$	$1.2\pm0.6\times10^{16}$
$N(HC_3N)$ [cm^{-2}][d]	$5.7\pm0.4\times10^{14}$	$5.6\pm0.4\times10^{14}$	$5.8\pm0.4\times10^{14}$	$4.6\pm0.3\times10^{14}$
$N(H^{13}CCCN)$ [cm^{-2}][d]	$1.5\pm0.1\times10^{13}$	$4.2\pm0.2\times10^{13}$	$1.4\pm0.1\times10^{13}$	$3.1\pm0.2\times10^{12}$
$N(HC_3N)/N(H^{13}CCCN)$[e]	37.7±0.4	13.3±0.13	43.4±0.4	146.0±1.4

[a]Position offsets in arcminutes from the Sgr B2 (M) position: $(\alpha,\ \delta)_{1950} = (17^h44^m10.5^s,\ -28°22'05'')$.
[b]Total integrated intensities $\int T_R^*\ dV\ (=\int T_A^*/\eta_B\ dV$, where η_B is the beam efficiency in §2) of the observed transitions.
[c]Total column densities derived using an excitation model.
[d]Total column densities derived assuming $\tau \ll 1$.
[e]Abundances ratios of HC_3N and $H^{13}CCCN$ for the case of $\tau \ll 1$. These values are lower limits and the errors are from the rotational temperature ranges only.

(1989). We have observed the 10−9 transitions of HC_3N and its ^{13}C substitutes ($H^{13}CCCN$, $HC^{13}CCN$, and $HCC^{13}CN$) in ~90 GHz and the vibrationally excited 12−11 (v_7=1) HC_3N transition in 109.44 GHz (Lovas 1992).The SIS receiver was employed and the typical system temperatures were about 150 K (SSB). The 1500 channel acousto-optic spectrometer with channel spacing of 0.69 MHz were used but the frequency resolution of the system was approximately 1.2 MHz. The HPBW and main beam efficiency are 50″ and 0.75, respectively, at 90 GHz. Five by nine point map was observed around Sgr2(M): $(\alpha,\ \delta)_{1950}=(17^h44^m10.5^s,\ -28°22'05'')$, with a grid of 45″. Spectra were taken in the position switching mode with the reference position $(\alpha,\ \delta)_{1950}=(17^h43^m00^s,\ -28°00'00'')$. The antenna temperature T_A^* quoted in this paper has been corrected for antenna and atmospheric losses by means of the standard chopper wheel method, but not for possible beam dilution. The typical rms of the spectra is about 30 mK.

III. RESULTS

In Figure 1 we show sample spectra of the 10−9 transitions of ground vibrational states HC_3N and its ^{13}C substitutes obtained toward (0, 0) and (0, 1.5′) from the Sgr B2 (M) position (§2). The $HC^{13}CCN$ and $HCC^{13}CN$ 10−9 transitions appear in the same spectrum together because their frequency difference is very small ($\Delta\nu \approx 9$ MHz). The column densities were determined by assuming optically thin emission using the standard expression (IGH) for the observed HC_3N and $H^{13}CCCN$ (10−9) lines, but the main isotope HC_3N abundances were also derived using an LVG model assuming the statistical equilibrium excitation. The abundances derived towards 4 selected positions are listed in Table 1. For the optically thin case we assumed the rotational temperature T_{rot}= 15-25 K (cf. Cummins, Linke, & Thaddeus 1986) and the errors of column densities in the table are from this temperature range. In using the LVG model we also apply ranges of physical parameters based on the previous results (Goldsmith *et al.* 1987; IGH): $n(H_2)=10^4$-10^5 toward the cores and 10^3-10^4 toward the more extended clouds and T_{kin}= 30-50 K. The LVG model results are shown in Figure 2 and also included in Table 1. In this calculation we have assumed that the fractional abundance of HC_3N is 2×10^{-9} relative to the total H_2 abundance and derive the total column densities large by more than an order of magnitude compared to the results assuming optically thin emission. The optically thin emission results are quoted as lower limits of the abundance.

Figure 3 shows the observed integrated intensity distributions of the HC_3N and $H^{13}CCCN$ 10−9 transitions. The intensity maps of $HC^{13}CCN$ and $HCC^{13}CN$ (10−9) show very similar distributions to that of $H^{13}CC$ CN. The solid lines display HPWs of the observed intensity. The HC_3N map indicates that the 2′N cloud may be spherical with a diameter of ~3.7 pc while the Principal Cloud is elongated along the declination (~4.5 pc in R.A. × 7.4 pc in Decl.). The optically thin $H^{13}CCCN$ line shows a peak intensity toward the (N) direction where hot dense clumps are thought to exist as leftovers after 'recent ' new star formations. It also shows an enhancement toward the 2′ north position where only very small number of molecules show increased intensities (Minh *et al.* 1998).

The vibrationally excited 12−11 (v_7=1) transition of HC_3N has been detected and its integrated intensity map is shown in Figure 4. The distribution is strongly concentrated around the (N) core and the HPW is ~0.9 pc in diameter. The upper level of the observed transition lies ~350 K above the molecular ground state. By applying a simple two level model we derive the vibrational temperature of T_{vib}= 113 K and the total column density of N(hot HC_3N) = 1.2×10^{15} cm^{-2}. However, the structure of the (N) core is very complicated and the excitation may be dominated by the infrared radiation of the (N) position (Goldsmith, Krotkov, & Snell

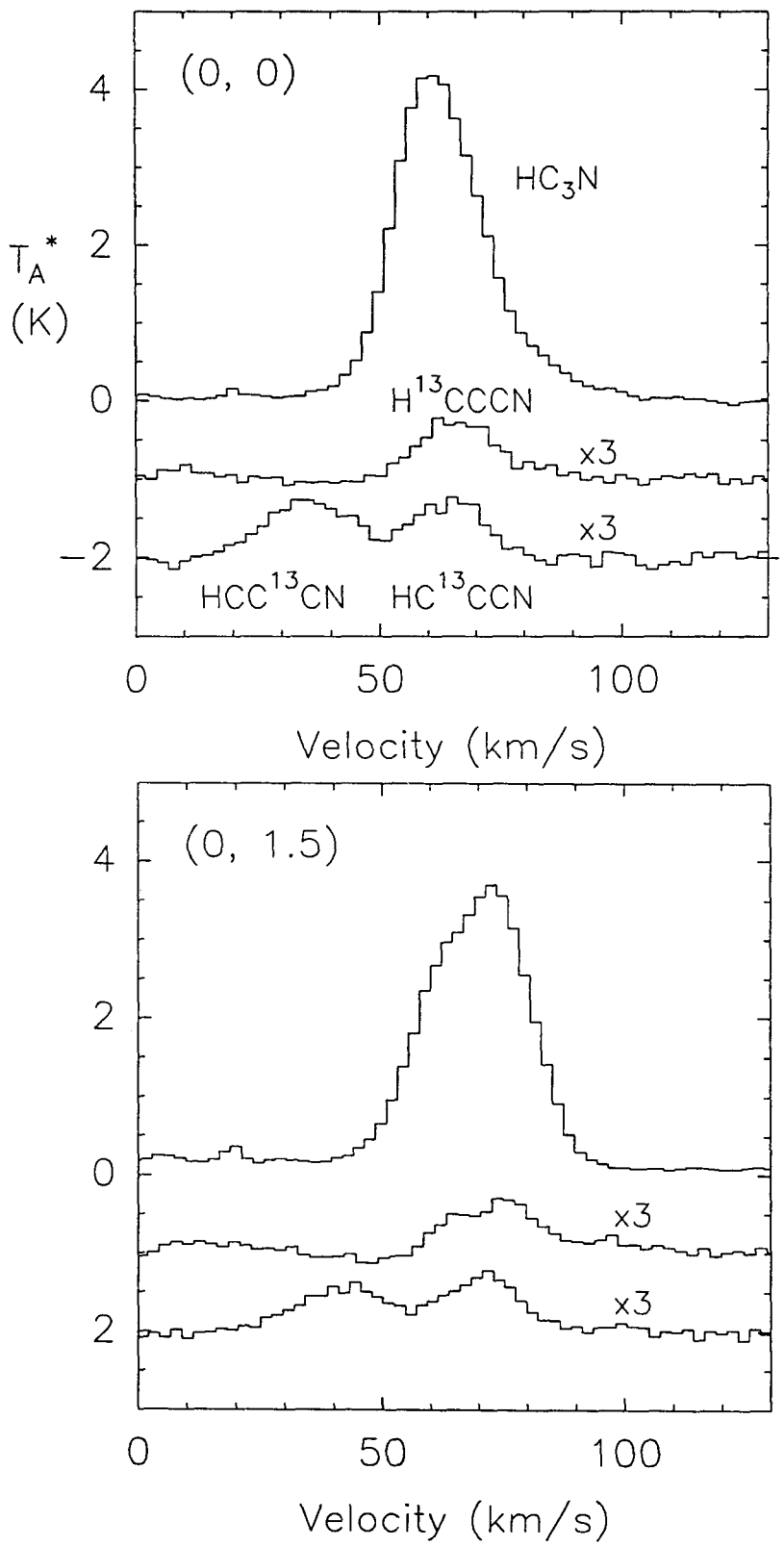

Fig. 1.— Sample spectra of the 10–9 transitions of HC_3N, $H^{13}CCCN$, $HC^{13}CCN$, and $HCC^{13}CN$ obtained toward (0, 0) and (0, 1.5′) from the Sgr B2 (M): $(\alpha, \delta)_{1950}=(17^h44^m10.5^s, -28°22'05'')$

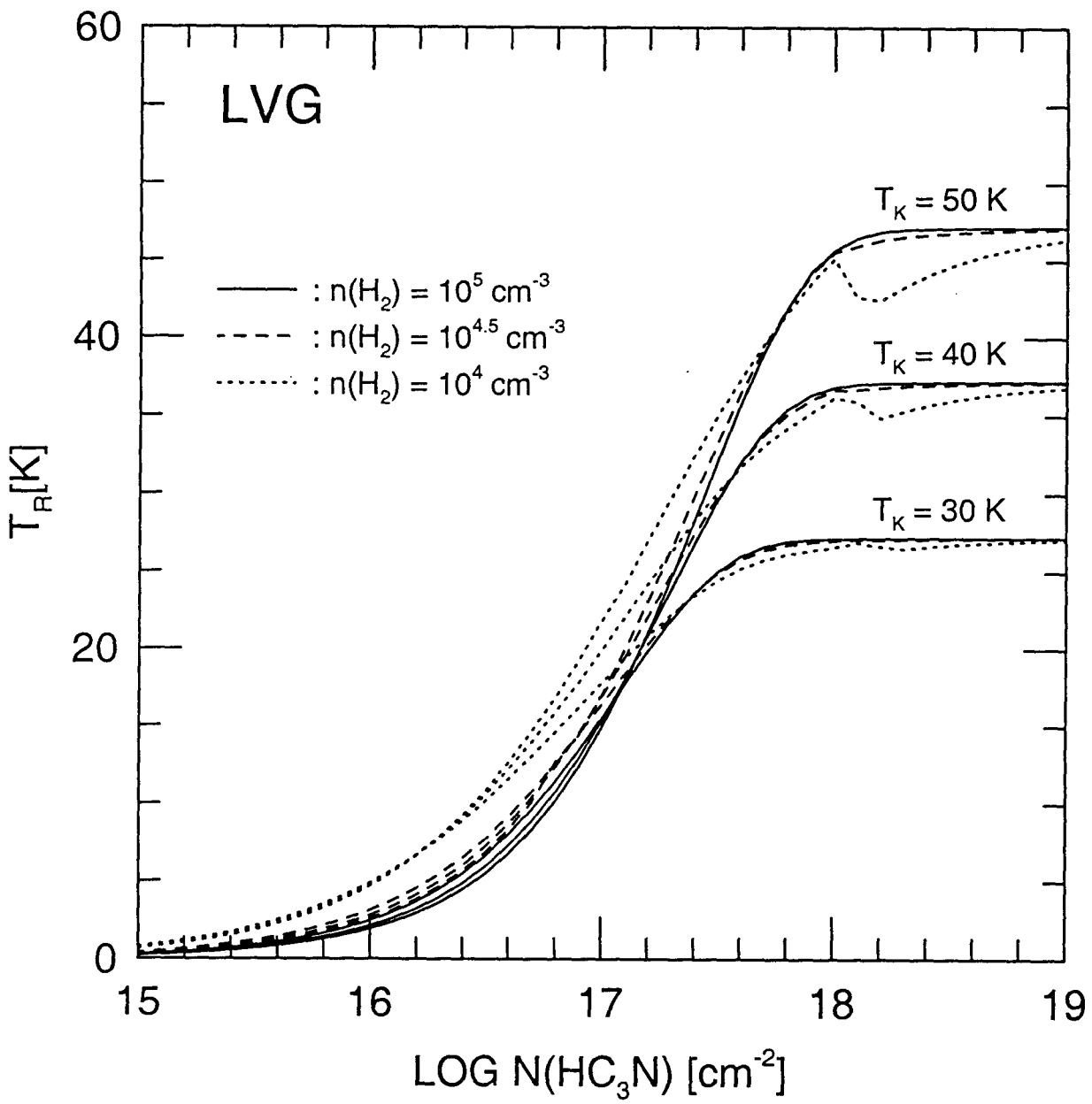

Fig. 2.— LVG model results for kinetic temperatures 30, 40, and 50 K.

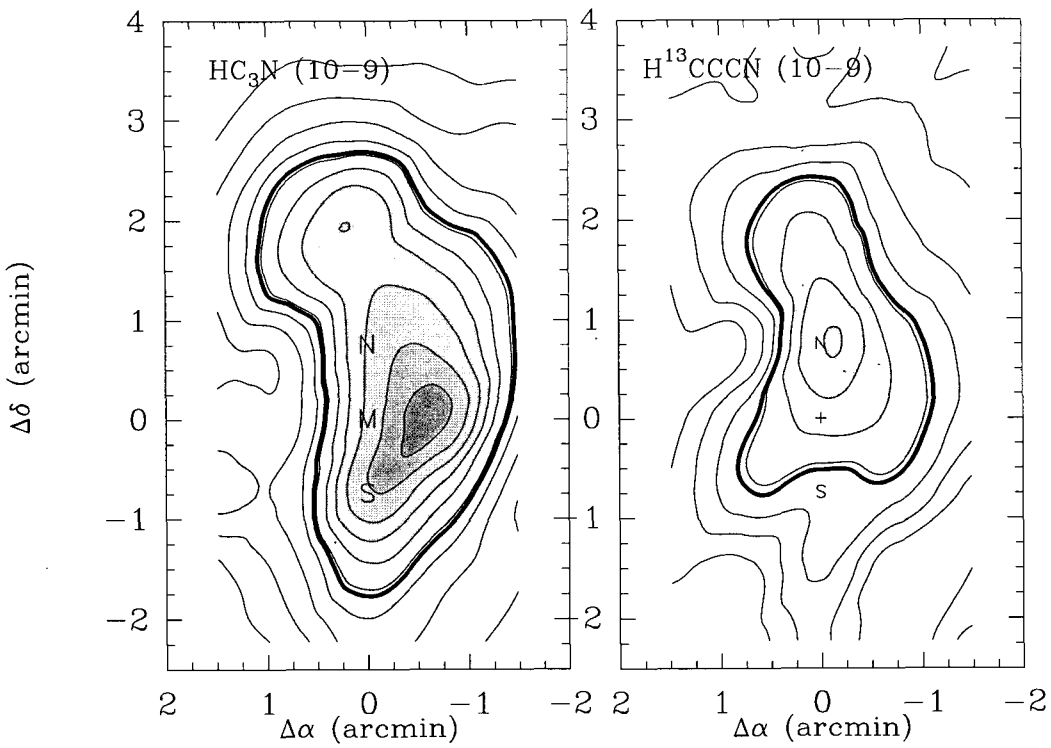

Fig. 3.— Integrated intensity maps of the 10–9 transitions of HC_3N and $H^{13}CCCN$. The contour level increases by 10 K km s^{-1} from 20 K km s^{-1} for HC_3N (10–9) and by 1 K km s^{-1} from 0.5 K km s^{-1} for $H^{13}CCCN$ (10–9). The thick solid lines are HPWs of the peak intensities.

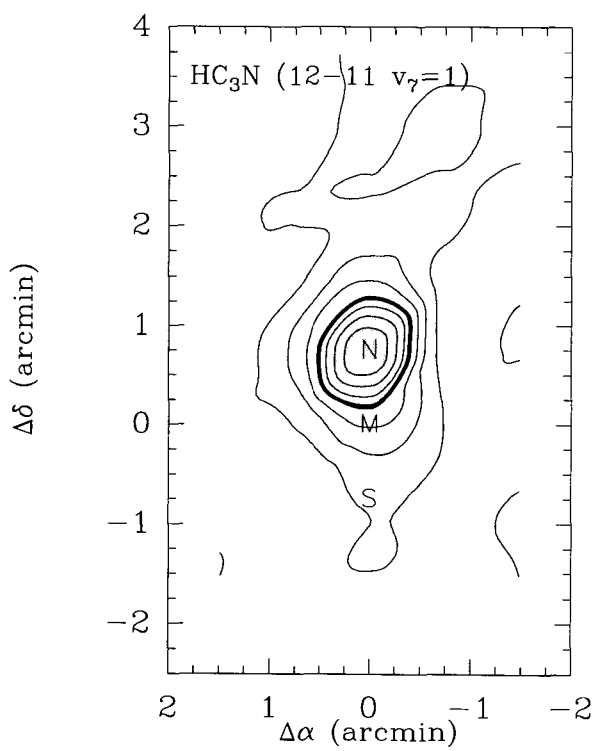

Fig. 4.— Integrated intensity map of the vibrationally excited 12–11 (v_7=1) HC_3N transition. The contour level increases by 1 K km s^{-1} from 0.5 K km s^{-1}. The thick solid line is the HPW of the peak intensity.

1986; IGH). The actual density and structure of the hot HC_3N in this region needs much further studies. Although the (M) core has similar compact HII regions and dense cores with the (N) core, no significant enhancement of the HC_3N 12−11 (v_7=1) transition has been found. Probably these two regions are in different evolutionary phases and, consequently, show different chemical properties. The chemical properties of the gas clouds in Sgr B2 show very interesting differences even in the regions of projected distances of a few parsecs.

Figure 5 shows the space-velocity map obtained along the declination at $\Delta\alpha$=0. The velocity gradient appears toward the north direction with a very similar pattern to that of HNCO (Minh *et al.* 1998). In the Principal Cloud region the line widths are somewhat consistent to 20-25 km s^{-1}, but it becomes large toward the 2′ N position which may suggest either some activities exist in this region or there is a new gas component with different V_{lsr} in the line of sight. To search for broad wing components which appear symmetric around 2′ N we have made a similar space-velocity map (Figure 6) along the direction connecting the (1.5′, 3.75′) and (-1.5′, 0.75′) positions. In regions near $\Delta\delta$ ~3 there is a weak component at 30 km s^{-1}, which is similar to the results for HCO_2^+ and HNCO (Minh *et al.* 1998). The column density of this component is about 5.4×10^{13} cm^{-2}. It has to be studied further whether this component is a separated cloud or the wing component of the 2′N cloud. Figure 7 shows velocity channel maps of the HC_3N (10−9) transition.

IV. DISCUSSIONS

The Sgr B2 molecular cloud is exceptionally dense and shows intense star formation activities, but the physical and chemical structures of Sgr B2 are still poorly known. Bally *et al.* (1988) and Hasegawa *et al.* (1994) suggest a shell structure around Sgr B2 and the formation of this cloud by the result of the collision between two molecular clouds. However, the formation of Sgr B2 is still controversial. The 2′N cloud may also suggest a collision between two gas clouds, which may lead to the formation of the next generation of massive stars. Only very small number of species have been found to show enhanced abundances at the 2′ N position (Wilson *et al.* 1996; Minh *et al.* 1998), and the physical and chemical properties of this region is still controversial. The observed HC_3N lines also show enhancements toward the 2′ N position compared to the extended envelope. If there exists a large-scale collapsing motion in this direction as suggested by the broad wing components of HNCO (Minh *et al.* 1998), the chemistry in this region can be initiated by a shock resulting from a possible collapse motion, which may release grain mantle material into the gas phase. In quiet gas phase HC_3N is formed via the reactions initiated by hydrocarbon ions and neutral nitrogens, which may have resulted an exceptionally large abundance of cyanopolyynes in the typical dark cloud TMC-1 (IGH). In shocked region the neutral-neutral reaction C_3H_3 + N, which may have a slight activation energy barrier, becomes important in the formation of HC_3N (Herbst 1983). In Orion-KL, the HC_3N abundance is also considerably larger in the plateau than in the quiet ridge cloud by a factor of about 20 (IGH). Thus the abundance of HC_3N is thought to be enhanced in the shocked region and the HC_3N results for the 2′ N region may suggest that some activities are occurring at this region. The 30 km s^{-1} component, which appears at the north-east direction, may also indicate a large scale collision if it is associated with the 2′N cloud. But it needs much further studies to confirm the structure of the 2′N cloud.

The abundances of the main isotope HC_3N appear to be similar to previous values obtained toward the (M) and (N) cores (IGH). We derive the lower limits of the abundance ratios $N(HC_3N)$ / $N(H^{13}CCCN)$ to be larger than 40 except the (M) and (N) cores where the main isotope lines must be optically thick. The $^{13}C/^{12}C$ ratio has been thought to be in the order of 20 at the Galactic center region, which may be resulted from an effective fractionation processes of ^{13}C at this region (see review by Taylor 1989). But because of the large optical depths toward (M) and (N) directions the abundances of the main isotope species can be underestimated largely. In fact we derive larger values of $N(HC_3N)$ / $N(H^{13}CCCN)$, even with lower limits of $N(HC_3N)$, than the cosmic abundance ratio of $C/^{13}C$ toward the 2′N region. Unlike the previous results, the small values of the $C/^{13}C$ isotopic abundance ratio may have resulted from the large optical depths of the main isotope species in the dense (M) and (N) cores. Our results suggest that the ^{13}C fractionation reactions may not be as effective as previous thoughts and the $C/^{13}C$ ratios may be much larger, by a factor of ≥ 2, than the values reported at the Galactic Center. The physical and chemical structures of Sgr B2 need to be studied much further to constraint the isotopic abundance gradients in the Galactic center.

V. CONCLUSION

We have observed the 10−9 transitions of HC_3N and its ^{13}C subsitutes ($H^{13}CCCN$, $HC^{13}CCN$, and $HCC^{13}CN$), and the vibrationally excited 12−11 (v_7=1) HC_3N transition toward the Sgr B2 molecular cloud. There exist several distinct clouds in Sgr B2 which have significantly different physical and chemical properties. The observed HC_3N lines show an extended emission toward the Principal Cloud to ~4.5 pc in R.A. × 7.4 pc in Decl. The optically thin $H^{13}CCCN$ line shows a peak intensity around the (N) core and we derive the total column density $N(H^{13}CCCN) = 4 \times 10^{13}$ cm^{-2}. The HC_3N lines show enhancement toward the 2′N Cloud compared to the extended envelope, which may have resulted from a large scale collapsing motion of the region. The hot component of HC_3N is strongly concentrated around the (N) Core and its HPW is ~0.9

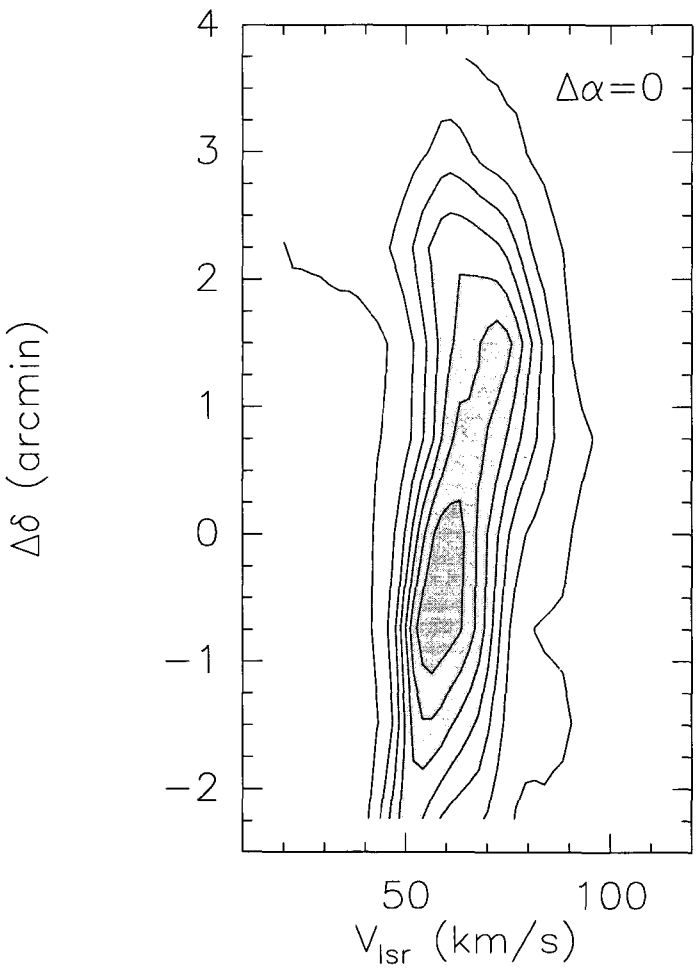

Fig. 5.— Space-velocity map of the HC_3N (10–9) transition along the declination at $\Delta\alpha$=0. The contour level increases by 0.6 K from 0.2 K.

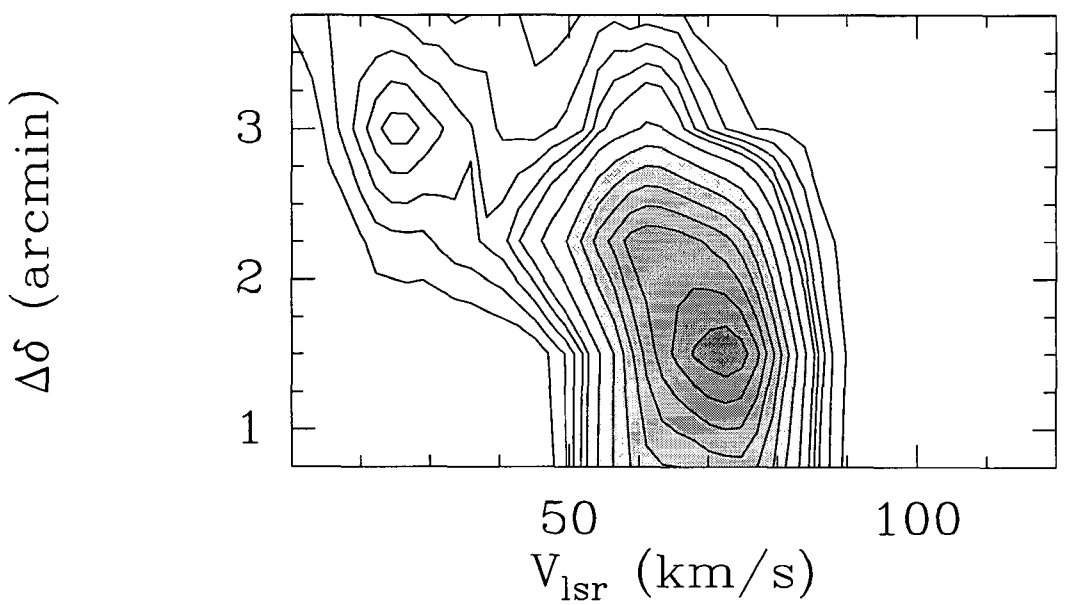

Fig. 6.— Same ad Figure 5 but along the direction connecting the (1.5′, 3.75′) and (-1.5′, 0.75′) position. The contour levels increase by 0.1 K from 0.2 K to 0.7 K and then increase by 0.3 K.

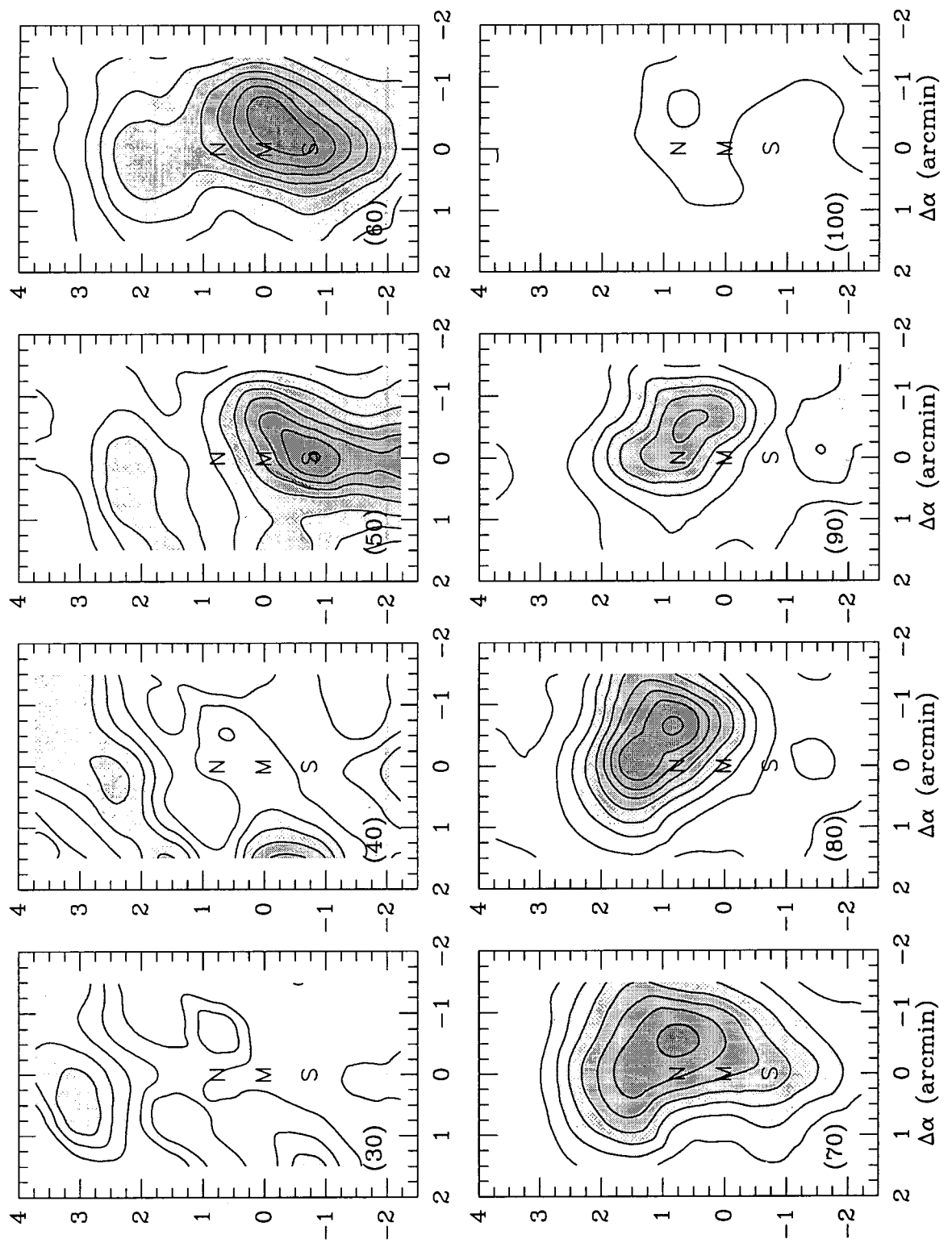

Fig. 7.— Velocity channel maps of the HC_3N (10−9) transition. The central velocities are shown in the bottom-left corner. The contours were derived by integrating ±5 km s^{-1} from the central velocity.. The lowest contour levels are 1 K km s^{-1}. The levels increase by 1 K km s^{-1} for the velocity channels of 30, 40, 90, and 100 km s^{-1}, 3 K km s^{-1} for 50 and 80 km s^{-1}, and 5 K km s^{-1} for 60 and 70 km s^{-1}.

pc in diameter. We derive lower limits of the abundance ratios $N(HC_3N)/N(H^{13}CCCN)$ to be larger than 40 except the (M) and (N) cores. The fractionation processes of ^{13}C at this region may not be as effective as previously reported.

ACKNOWLEDGEMENTS

We are very grateful for the excellent support by the SEST and ESO staffs in making observations and reducing data.

REFERENCES

Bally, J., Stark, A.A., Wilson, R.W., & Henkel, C. 1988, ApJ, 324, 323.

Booth, R.S., Delgado, G., Hagstrom, M., Johansson, L.E.B., & Murphy, D.C. 1989, A&A, 216, 315.

Cummins, S.E., Linke, R.A., & Thaddeus, P. 1986, ApJS, 60, 819.

Goldsmith, P. F., Krotkov, R., & Snell, R. L. 1986, ApJ, 299, 405.

Goldsmith, P.G., Snell, R., Hasegawa, T., & Ukita, N. 1987, ApJ, 314, 525.

Gordon, M.A., Berkermann, U., Mezger, P.G., Zylka, R., Haslam, C.G.T., Kreysa, E., Sievers, A., & Lemke, R. 1993, A&A, 280, 208.

Hasegawa, T., Sato, F., Whiteoak, J.B., & Miyawaki, R. 1994, ApJ, 429, L77.

Herbst, E. 1983, ApJS, 53, 41.

Irvine, W.M., Goldsmith, P.F., & Hjalmarson, Å. 1987, "Interstellar Processes", eds. D.J. Hollenbach & H.A. Thronson, Jr., Reidel: Dordrecht, p. 561 (IGH).

Lovas, F.J. 1992, J.Phys.Chem.Ref.Data, 21, 181.

Minh, Y.C., Haikala, L., Hjalmarson, Å. & Irvine, W.M. 1998, ApJ, 498, 261.

Minh, Y.C. & Hjalmarson, Å. 1998, Adv. Sp. Res. submitted.

Nummelin, A. et al. 1998, A&AS, submitted.

Scoville, N.Z., Solomon, P.M., & Penzias, A.A. 1975, ApJ, 201, 352.

Taylor, D. 1989, Thesis, Univ. of Massachusetts.

Thronson, H. A. & Harper, D. A. 1986, ApJ, 300, 396.

Wilson, T.L., Snyder, L.E., Comoretto, G., Jewell, P.R., & Henkel, C. 1996, A&A, 314, 909.